

Article

Methods of Assessing the Effectiveness of Filter Elements in Power Electronics

Michał Borecki *  and Jan Sroka

Institute of Theory of Electrical Engineering, Warsaw University of Technology, 00-662 Warsaw, Poland; j.sroka@pw.edu.pl

* Correspondence: michal.borecki1@pw.edu.pl

Abstract: Newly constructed devices must meet a number of requirements in terms of the level of generated disturbances. To achieve an acceptable level in such devices, filters are installed—one of the cheapest ways to reduce interference in devices. One of the key elements of the filter that is responsible for the effectiveness of noise reduction are ferrites. Unfortunately, for various devices, an individual approach should be used in the selection of filters and, accordingly, ferrites. Due to the fact that ferrites from different manufacturers do not have standardized characteristics and information on their effectiveness, the selection of the right ferrite is a very time-consuming process. Therefore, this article will present the possibilities of quickly determining selected ferrite parameters in order to ensure the necessary level of noise reduction. For this purpose, assumptions from the CISPR 17 standard will be used. For selected types of ferrites, a large number of measurements were carried out in order to determine the optimal computational algorithm for adjusting ferrite characteristics to the designed conditions. The performance of these tests will be the basis for conducting tests on a larger number of ferrites, as well as for the development of possible standardization procedures.

Keywords: ferrite; radio emission; power electronics; filter; EMC; CISPR 17



Citation: Borecki, M.; Sroka, J.

Methods of Assessing the Effectiveness of Filter Elements in Power Electronics. *Energies* **2022**, *15*, 5061. <https://doi.org/10.3390/en15145061>

Academic Editor: Miguel Castilla

Received: 30 May 2022

Accepted: 3 July 2022

Published: 11 July 2022

Publisher's Note: MDPI stays neutral with regard to jurisdictional claims in published maps and institutional affiliations.



Copyright: © 2022 by the authors. Licensee MDPI, Basel, Switzerland. This article is an open access article distributed under the terms and conditions of the Creative Commons Attribution (CC BY) license (<https://creativecommons.org/licenses/by/4.0/>).

1. Introduction

There are some problems with the development of technology. One of such problems are the disturbances and electromagnetic radiation that affect human health and the environment [1–4]. In order to counteract the negative effects of such an impact, research is conducted to enable the development of materials that absorb electromagnetic waves [5]. In order to reduce the level of electromagnetic disturbances, filters are used in the devices. The most common materials that absorb electromagnetic waves in filters are ferrites. The advantages of ferrites are profitability, excellent magnetic losses, and work stability [6].

Conventional ferrite has higher resistivity, dielectric properties, and transmittance at higher frequencies than magnetic alloy materials. Consequently, ferrites are widely used in the high-frequency field [7]. Various materials have been used to make ferrite cores [8–13].

Ferrites are characterized by high-saturation magnetization, high resistance, and high chemical stability [14,15]. Nickel–zinc ferrite is used in power engineering in devices such as transformers [15,16].

As can be seen from the above, there are many different types of ferrites and many ferrite manufacturers, but there is no standard or standard that requires ferrites. Therefore, not all manufacturers include the performance characteristics of ferrite; it is not always possible to specify the frequency range for which a ferrite is effective, which ferrite components affect its parameters, etc. This leads to the fact that choosing ferrite for the filter often requires determining its effectiveness through multiple measurements and multi-iterative selection of the correct form of such ferrite, which is very time-consuming.

During such selection, the main emphasis is placed on improving the dielectric and magnetic properties [16–18].

When designing filters, it is important to assess the effectiveness of damping at the prototype stage, through simulations [19–21].

Therefore, in order to accelerate the selection process, this paper proposes a method of determining the form of ferrite which will be most effective in suppressing electromagnetic interference.

Ferrite plays an important role in defining the parameters of filters that are used at every stage of the life cycle of the device and the facility where such devices are installed [22–24]. In order to analyze the method of increasing the effectiveness of selected types of ferrites, the CISPR 17 standard was used [25].

The first section of this article contains an introduction that justifies the need to perform research enabling the acceleration of the selection of ferrite with appropriate parameters with reference to the bibliography. Section 2 presents the parameters of the analyzed ferrites for which the measurements were made. Section 3 presents the measurement results for various options using the Gauss meter and the quasipeak (QP) and average (AV) detectors. Section 4 proposes a mathematical model of the method of accelerating the selection of the appropriate form of ferrite, which will be the most effective in the context of electromagnetic interference suppression. Section 5 summarizes the research carried out.

2. Materials and Methods

As is well-known, ferrites can be produced from various materials. Each manufacturer has its own designation of these materials. Detailed parameters of these materials are not provided. Most often (in the better case), it is the magnetic permeability characteristic of frequency. This parameter allows you to take into account the change in the magnetic field over time. At the same time, in order to reflect the influence of the environment on the phase deviation of the magnetic induction vector B in relation to the magnetic field strength vector H , a complex parameter of magnetic permeability is used according to Equation (1):

$$\mu = \mu' - j\mu'' \quad (1)$$

where μ' is the real part, meaning the inductive component, and μ'' is the imaginary part, meaning the resistive component.

Some manufacturers just provide a complex parameter of magnetic permeability. This parameter is dedicated to a specific core; therefore, it is impossible to transfer this parameter to a larger range of ferrites. Here is a helpful parameter AL that can be used for larger ranges of cores. The discussed parameter determines the inductance of the coil, which depends on the number of turns of the shuttle. This parameter is specified in the format of a certain range of values. Another level of accuracy in providing data by some manufacturers is in the provision of the change-from-frequency characteristic of the composite parameter of magnetic permeability. At the same time, the best solution is for manufacturers to provide the characteristics of the inductive component and the resistive component. However, if the analysis covers a specifically selected ferrite or a device for which a specific ferrite should be selected, in this case, using a vector circuit analyzer, the ferrite impedance components can be determined using one of the three methods. Then, using the Equations (2) and (3), the obtained values can be converted into components of the complex parameter of magnetic permeability:

$$\mu' = l/(\mu_0 S N^2) \dot{L} \quad (2)$$

$$\mu'' = l/(\mu_0 S N^2) \dot{R}/(2\pi f) \quad (3)$$

where S —ferrite cross-sectional area; l —ferrite magnetic field line length; μ —vacuum permeability; N —number of turns; f —magnetic field frequency; L —inductance; and R —resistance. This article considers three different ferrites according to the characteristics shown in Figures 1–3.

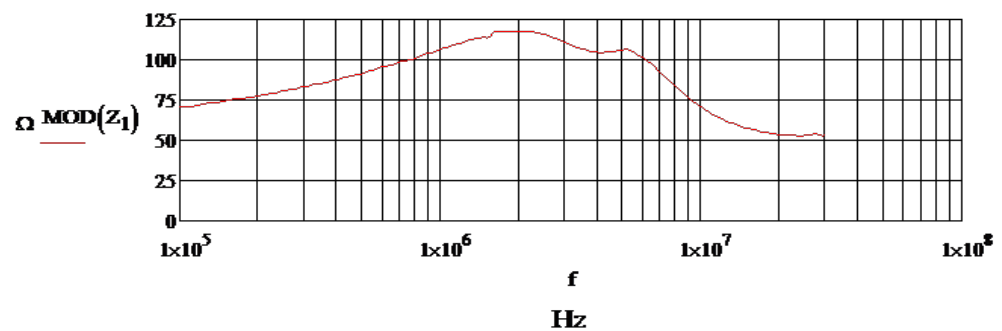


Figure 1. Characteristics of ferrite No. 1.

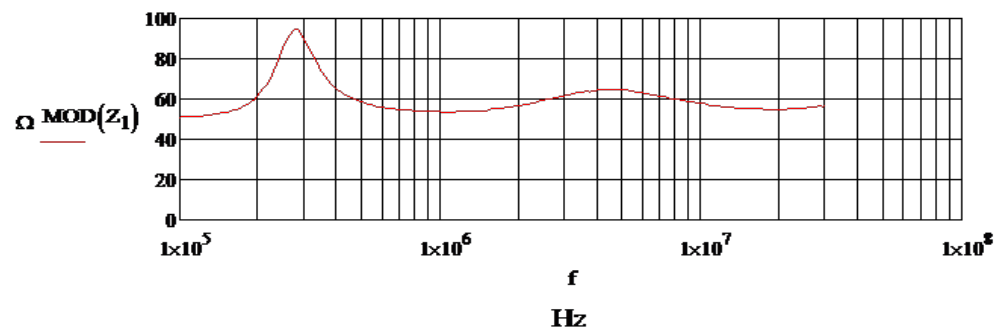


Figure 2. Characteristics of ferrite No. 2.

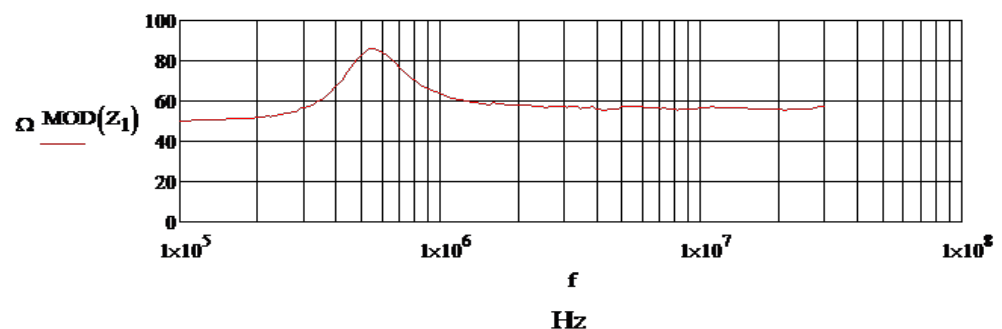


Figure 3. Characteristics of ferrite No. 3.

The most common type of ferrite was selected. The assumption is that testing this type of ferrite will enable the transfer of the obtained results to other types of ferrites. The Figures 1–3 shows the characteristics of ferrites that will be analyzed in this article, assuming no additional turns on these ferrites (initial state). Moreover, the discussed ferrites will be adapted to the form which will ensure the greatest effectiveness of the work of these ferrites.

3. Results

As part of the analysis of the parameters of the selected ferrites, in the first stage, the base (based on calculations) value of the ferrite coils was determined. The base value of the coils must theoretically provide effective damping. We will explain in the following section whether this is actually the case. For ferrite no. 1, the base value of the coils was calculated at the level of 22 (Figure 4).

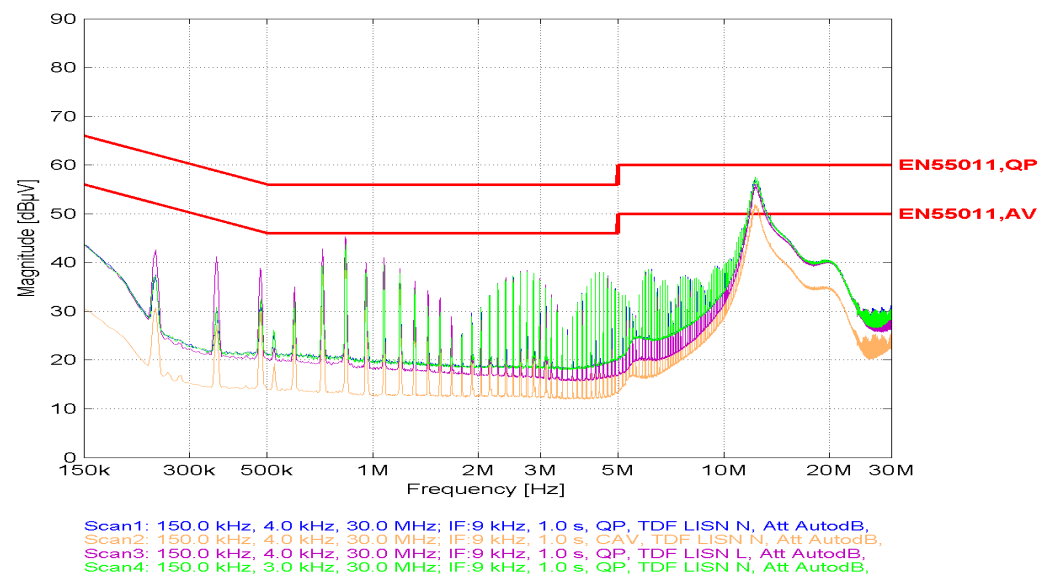


Figure 4. Attenuation level for ferrite No. 1 with the number of coils at 28 pcs.

In the case of using 25% more than the calculated base number of turns, we can see that this enables effective damping. Confirmation of this is shown in Figure 4.

As can be seen, the attenuation exceeds the allowable limit in the range of 12 to 15 MHz. Due to the frequency range in which the considered ferrite interacts, this range is omitted in this analysis. At the same time, it should be noted that reducing the damping value in this frequency range will be possible based on the use of additional capacities.

In the event of a decision regarding the possibility of reducing the number of turns, it was decided to perform tests for 26 turns, i.e., at the level of +15% about the base number of turns. At this point, it should be noted that reducing the number of turns still allows one to “stay” within the acceptable limits. However, it can be seen that reducing the number of turns and approaching the baseline computational number of turns allows an increase in the “safety buffer” over the indicated limit. In the case of reducing the number of turns by 2 pcs (Figure 5), above the computational level of the number of turns, the attenuation level drops by about 3 db (from 45 dB to 42 dB).

Therefore, calculations were performed for the base computational level of the number of turns.

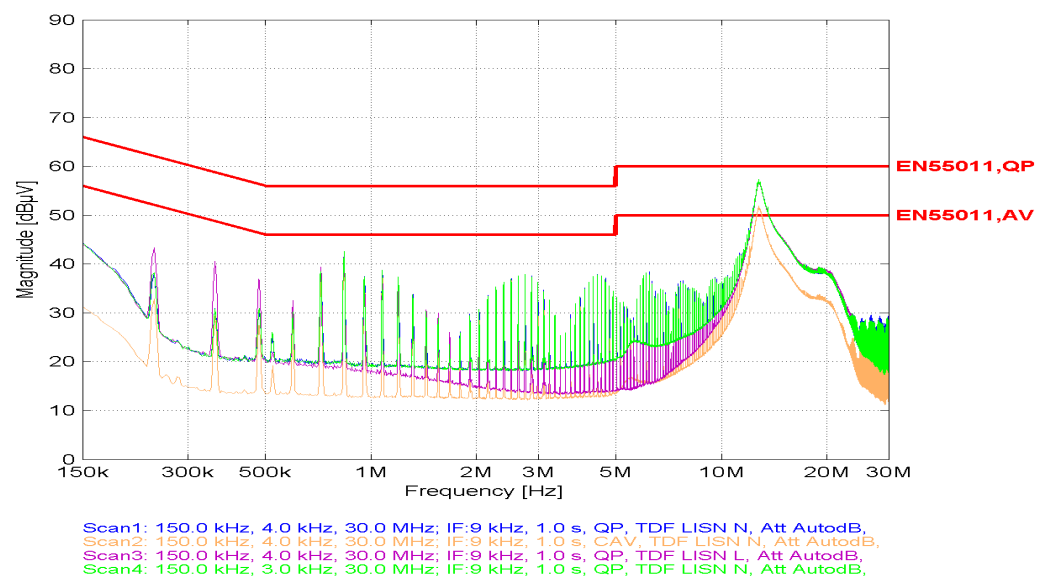


Figure 5. Attenuation level for ferrite No. 1 with the number of coils at 26 pcs.

It should be noted here that the calculations show that the basic number of turns necessary for effective attenuation is 22. This assumption is because we assume an attenuation buffer at the level of 10 dB. Only for values exceeding the permissible limits do we assume a higher level of 15 dB. It is this increased level of attenuation that causes the computational number of turns to increase from 19 to 22. This attenuation interval requires several turns in the range 21,418–21,273 (Figure 6). In the case of fractional values, we assume that we round to the higher value to increase the buffer, ensuring the expected result.

Going back to the entire frequency range (100 kHz–30 MHz), which consists of 201 points, the results for ferrite No. 1 were obtained in the range of 11.979–18.657 turns. Due to the above, the base number of turns was adopted at the level of 22.

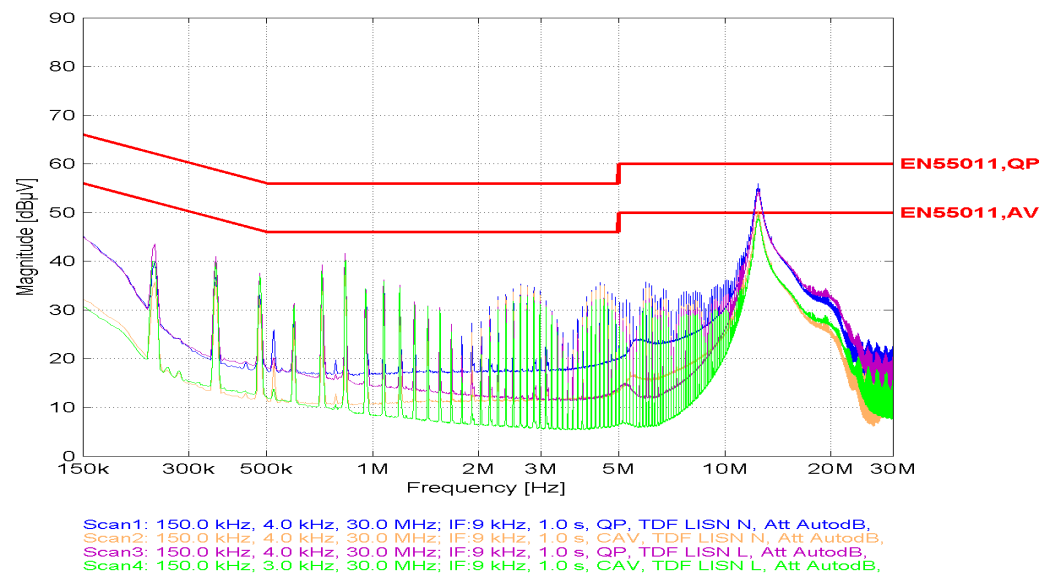


Figure 6. Attenuation level for ferrite No. 1 with the basic number of coils (22 pcs.)

The calculations show that reducing the number of turns from 26 to 22 does not introduce major changes in the attenuation. This level in the maximum range is about 42 dB.

Therefore, we continued to reduce the number of turns from 22 pcs to 18 pcs, which is below 15% from the baseline. It should be mentioned that the characteristics of the analyzed ferrite are different than the characteristics of the other two considered ferrites, which may also affect the attenuation results and the calculated number of turns. The results depend on the frequency range over which the damping has to be performed. Usually, this is an uneven characteristic (Figure 7).

As can be seen, in the case of reducing the number of turns below the base computational level of turns, the difference between the allowable limit and the maximum attenuation value slightly decreases (by about 1 dB). Therefore, it was decided to reduce the number of turns to 15 pcs.

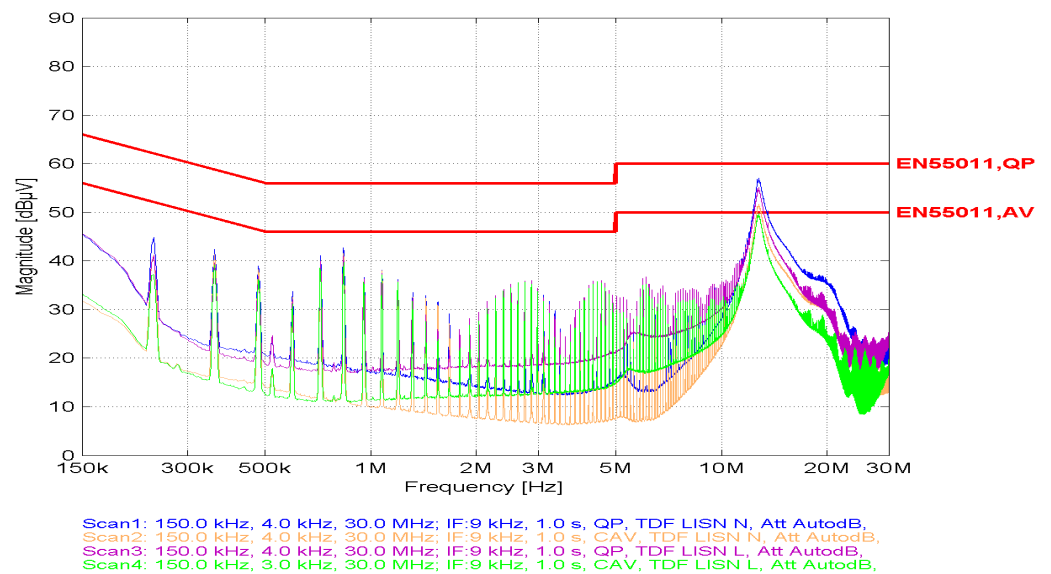


Figure 7. Attenuation level for ferrite No. 1 with the number of coils at 18 pcs.

When analyzing this case in terms of maximum values below the limit, no significant changes were observed. At the same time, in the frequency range above 10 MHz, attenuation values were obtained that are below the limit. However, further studies on the subsequent reduction in the number of turns showed that this case should be excluded from the analysis due to the probable measurement error. The obtained results for 15 coils allowed to carry out the tests for a greater step of changing coils (by 5 pcs.) (Figure 8).

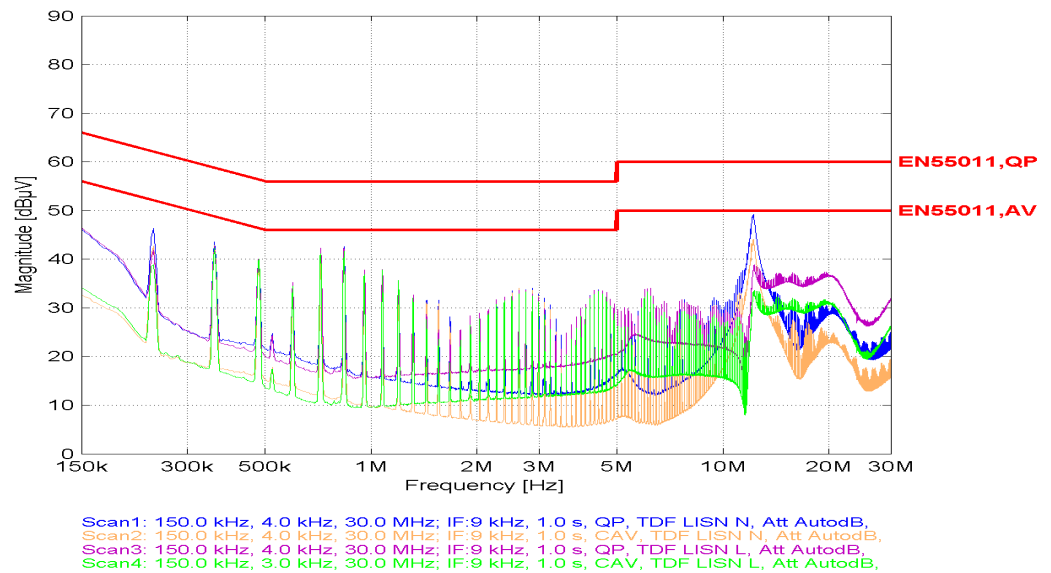


Figure 8. Attenuation level for ferrite No. 1 with the number of coils at 15 pcs.

In the case of tests for 10 pieces of coils, it can be seen that the maximum values in the frequency range of 12–15 MHz exceed the defined AV limit by approx. 2 dB.

Therefore, an attempt was made to carry out tests for 12 pieces of coils (Figure 9).

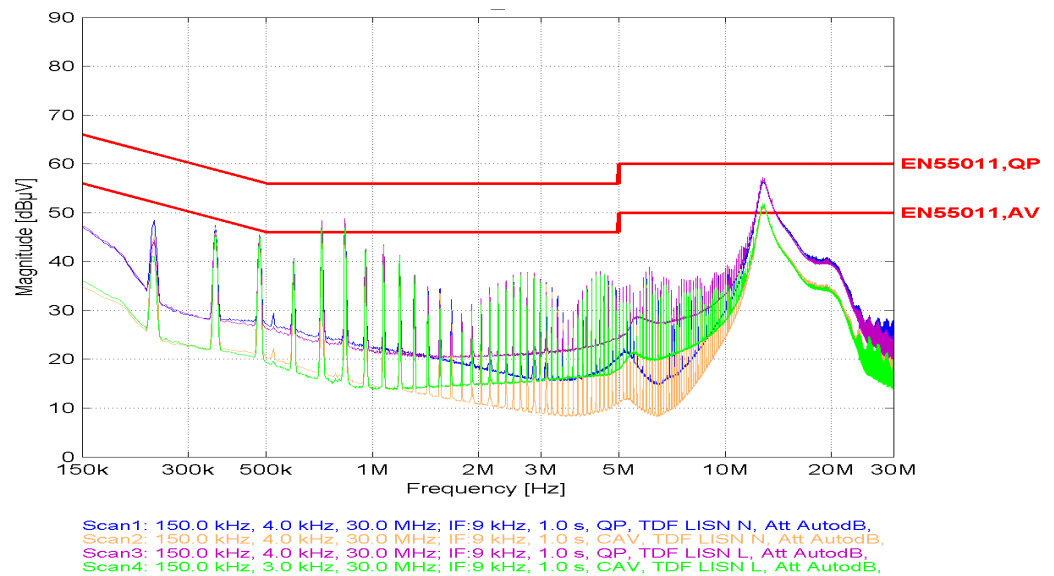


Figure 9. Attenuation level for ferrite No. 1 with the number of coils at 10 pcs.

As you can see in the case of 12 coils, the maximum attenuation values in the range we are interested in are at a level comparable to the AV limit (Figure 10). In the case of ensuring the absolute effectiveness of ferrite operation, it was proposed to increase the number of turns by 1 item and to set the final effective number of turns at the level of 13 items. The experimentally obtained value for ferrite No. 1 is nine items lower than the calculated value, i.e., by over 40%.

Therefore, based on the conducted research, it was found that there is a need to correct the formula for the calculation of the number of turns. For this purpose, the use of a correction factor of 0.59 has been proposed. In order to clarify/confirm the value of this coefficient, further tests were carried out for ferrites with different characteristics. The implementation of the above activities will enable:

- Precise selection of the number of turns, which is synonymous with ensuring better performance characteristics of the device;
- Saving materials in the field of making coils;
- Reducing the size of ferrite devices or using the freed space for other purposes.

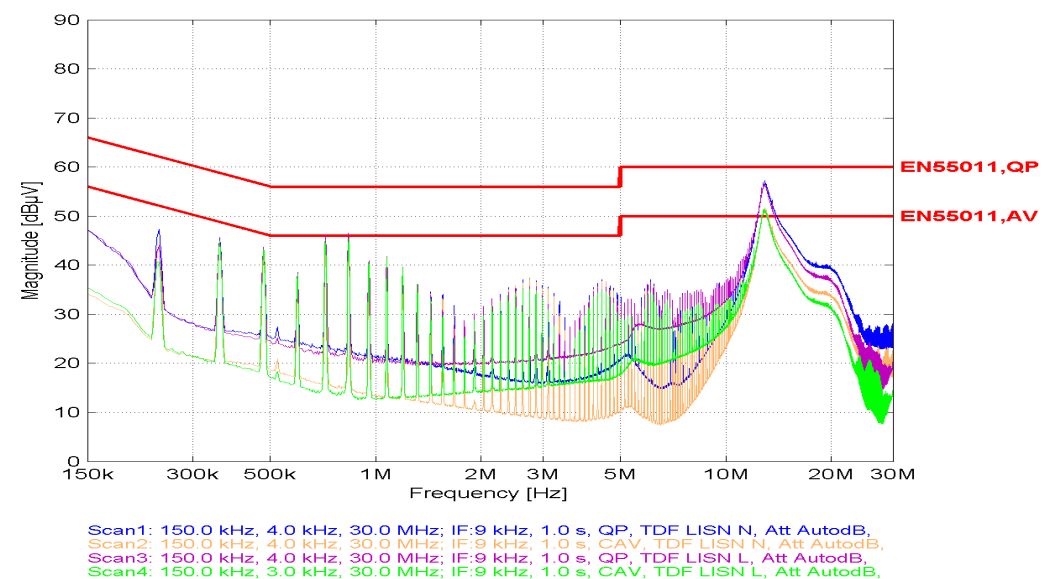


Figure 10. Attenuation level for ferrite No. 1 with the number of coils at 12 pcs.

For this purpose, calculations for ferrite No. 2 were performed to determine the computational number of turns. The basic design number of turns is 39 pcs. At the same time, the range of changes in the number of ferrites for different frequencies is from 17.222 to 38.966. At this point, it should be noted that the approach to the attenuation level is similar to that of other ferrites. However, due to the different characteristics of the analyzed ferrite, the change in the assumed attenuation level in the 500 kHz–1 MHz range does not in any way affect the value of the base computational number of turns. It should be noted here that in the 500 kHz–1 MHz range, with the attenuation to be compensated (reduced) by 10 dB, the number of turns is 18, while if the attenuation is increased to 15 dB, the number of turns increases to 27, and in the case of 20 dB, it is 36 pcs. However, if it is necessary to compensate the attenuation level at the level of 20 dB in the whole frequency range, 77 pcs coils are needed.

To confirm the trends defined for the previous ferrite no. 1, tests were carried out taking into account the increase (Figure 11) and decrease (Figure 12) of the number of turns by 1 piece, which is 2.5% of the base number of turns.

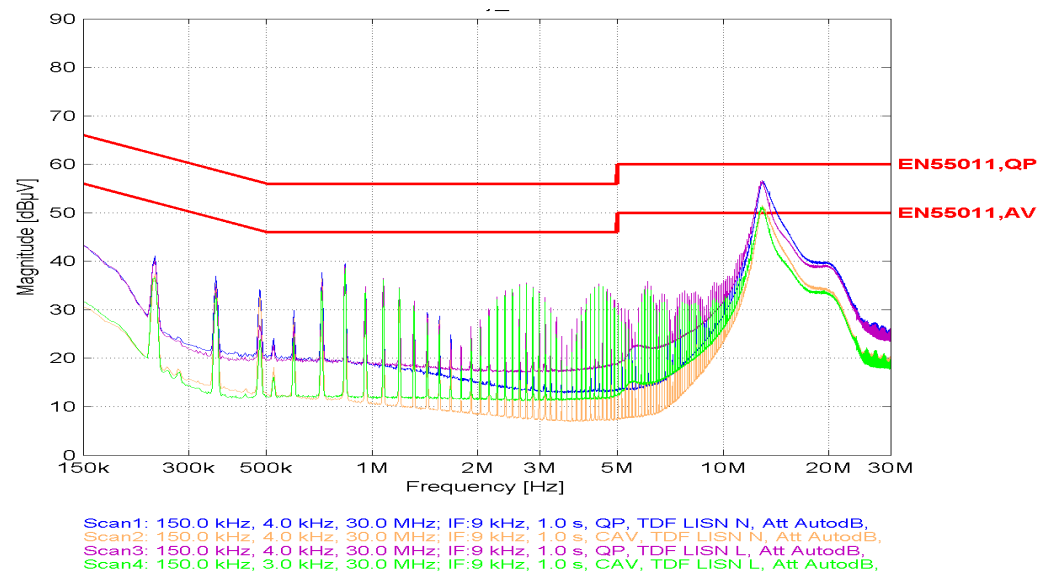


Figure 11. Attenuation level for ferrite No. 2 with the number of coils at 38 pcs.

In the case of reducing the ferrites, it can be seen that the obtained level of attenuation decreases and is far from the set limit. On the other hand, in the case of increasing the number of ferrites above the base computational level, the level of attenuation increases dramatically, but remains within the acceptable values. At the same time, when increasing by a few more ferrites, it confirms the tendency of no justification for increasing the number of turns above the base computational level. In the performed measurements, the step was the same, but the difference in the maximum attenuation level in the 500 kHz–2 MHz frequency range between the analyzed cases is 5 dB.

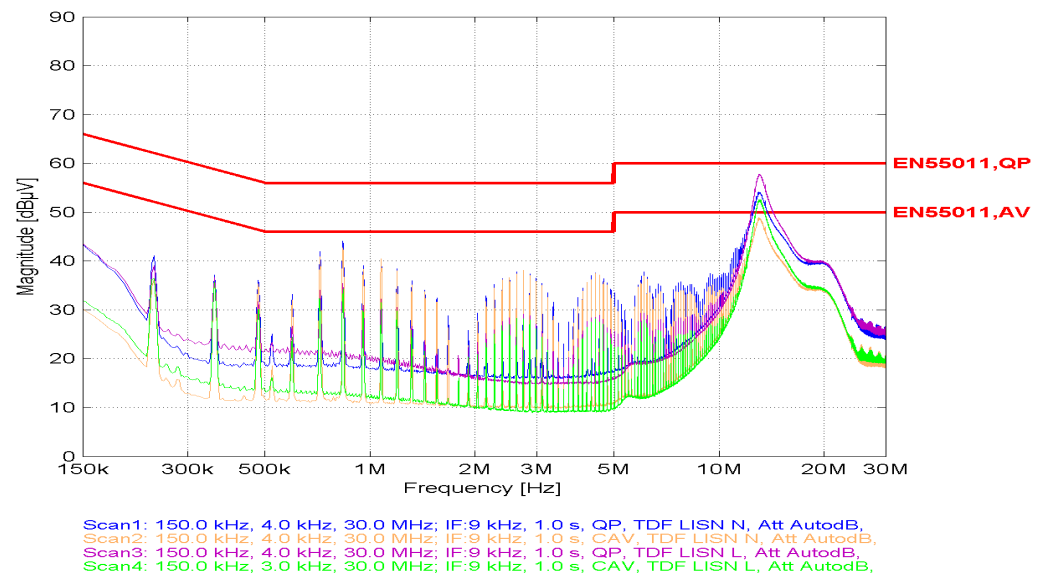


Figure 12. Attenuation level for ferrite No. 2 with the number of coils at 40 pcs.

In the next step, tests were carried out to reduce the number of turns to 30 pcs (Figure 13). Even such a reduction in the number of turns provides effective damping and a reserve for further reduction of turns.

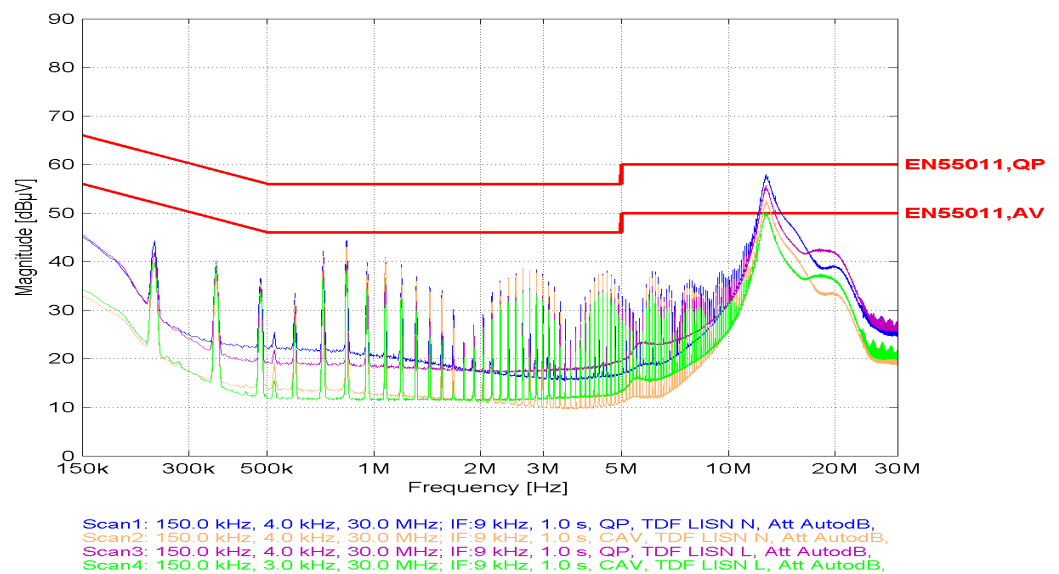


Figure 13. Attenuation level for ferrite No. 2 with the number of coils at 30 pcs.

The optimal number of turns for a given ferrite no. 2 is 28 pcs (Figure 14). This means that the design level of the ferrite number can be reduced by 11 pcs. Without any impact on the attenuation efficiency. The reduced number of turns for ferrite No. 2 (11 pcs) is greater than that of ferrite No. 1 (9 pcs). However, in percentage terms, greater reductions in the number of turns were obtained in the case of ferrite No. 1.

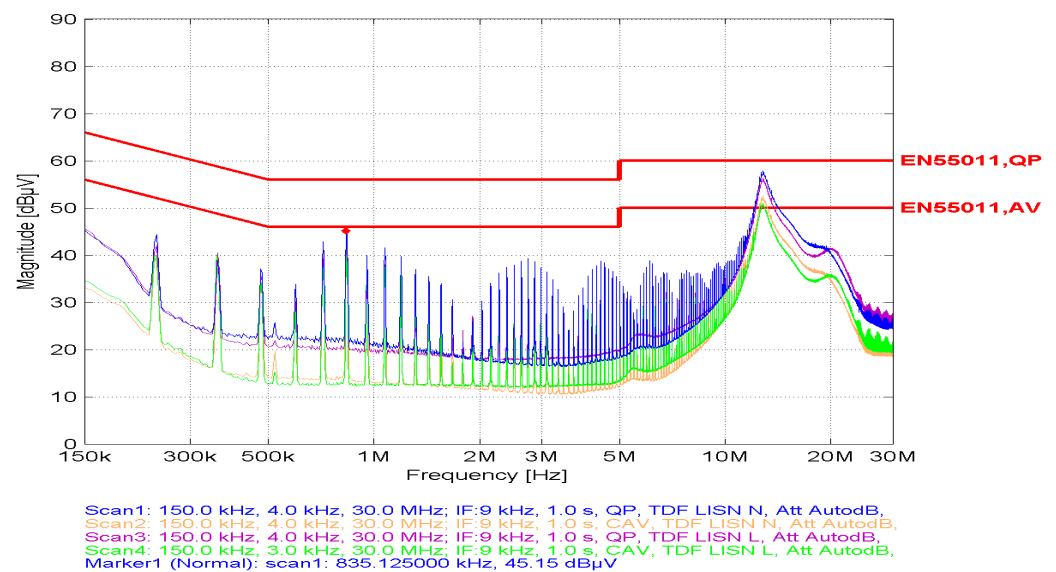


Figure 14. Attenuation level for ferrite No. 2 with the number of coils at 28 pcs.

4. Discussion

Looking at the results for all ferrites, you can see the peak of the attenuation amplitude above 10 MHz. This jump is due to the capacities. On the other hand, in terms of ferrite efficiency analysis, the most interesting range is below 10 MHz. Taking into account the results of previous research, it was decided to research in the field of ferrite no. 3 (Figure 15). The base computational number of turns in the entire frequency range ranged from 17.009 to 39.384. Therefore, taking into account the assumptions in the previous tests, the base computational level of turns of 39 pcs was adopted. At the same time, in the frequency range with the maximum attenuation level and taking into account the attenuation compensation requirement at the level of 15 dB, the computational number of coils was obtained at the level of 28 in this range. Taking into account the results of previous tests, the following procedure was adopted:

- 1. The change in the number of turns takes place in the direction of decrease about the calculated level;
- 2. The step of change is 10%.

Due to the above, calculations were made for 35 pieces of coils. The obtained results indicate that in the case of using the number of turns at the level of 34, which is 12.5% less than the base calculation, it is necessary to maintain the permissible limit of variability.

Therefore, differentiation in the application of the reducing coefficients depending on the type of ferrite was adopted. At the same time, this universal coefficient la is 0.88. However, the dedicated factor, depending on the type of material the ferrite is made of, is one for ferrite No. 3, 0.9 for ferrite No. 2 (you need to multiply the universal one for the dedicated one), and 0.8. for ferrite No. 1. Taking the above into account, in order to determine the number of turns for each type of ferrite, the following formula was proposed:

$$N_p = 0,88\dot{S}N_b \quad (4)$$

where: N_p —recalculated number of ferrite turns; K —material factor of ferrite (in the present article for ferrite No. 1— $K = 0.8$); and N_b —basic number of ferrite turns resulting from the formula $N_b = \sqrt{(L/AL)}$, where L is the inductance coils and AL is the coefficient corresponding to the effective permeability μ_e .

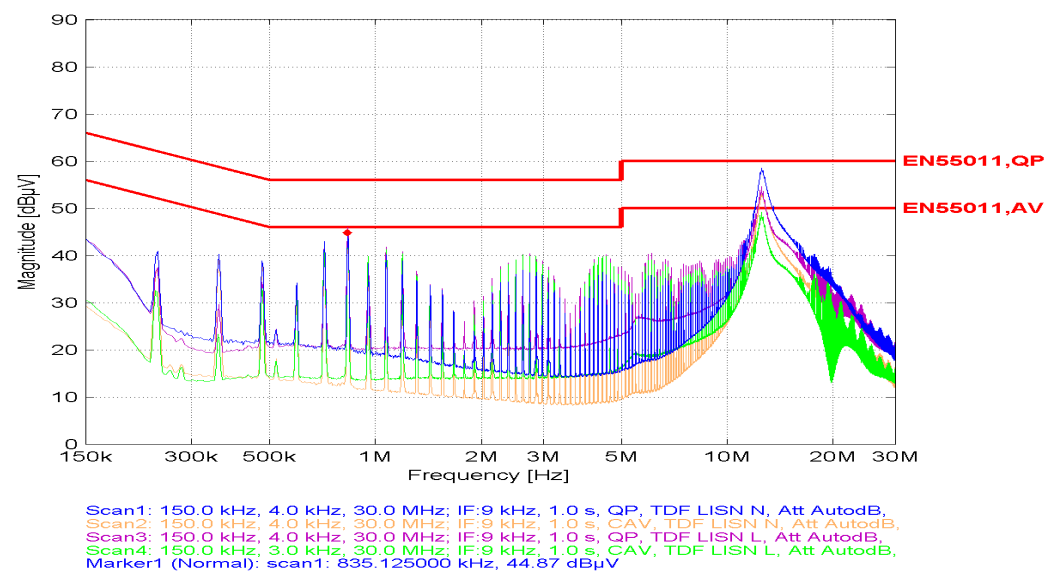


Figure 15. Attenuation level for ferrite No. 3 with the number of coils at 35 pcs.

5. Conclusions

In this article, selected characteristics of ferrites and the possibilities of accelerating the adaptation of their characteristics to the appropriate level of interference are considered. The adaptation criterion is the ease of the calculations made and the ease of changing the characteristics to the expected needs. As part of this article:

- The characteristics of three different ferrites were compared;
- Measurements were made for various ferrite modifications in terms of the change in the number of turns;
- A solution was proposed to enable the determination of the optimal number of turns at the design stage to ensure the speed of selection of the appropriate ferrite modification and material saving.

The obtained results were made with a large number of measurements for various cases. Therefore, for certain types of ferrites, the obtained results can be used in practical solutions. In addition, the conducted research opens the possibility of developing appropriate calculation algorithms for a larger number of ferrite types and possible future normalization of the ferrite characteristics adjustment to the designed conditions.

The mathematical model proposed in this article, ensuring the greatest possible limitations of electromagnetic interference in devices, will enable the filter design time to be shortened, which also translates into the design time of the device.

Author Contributions: Conceptualization, M.B. and J.S.; methodology, M.B.; software, M.B. and J.S.; validation, M.B. and J.S.; formal analysis, M.B.; investigation, M.B. and J.S.; resources, M.B. and J.S.; writing—original draft preparation, M.B.; writing—review and editing, M.B.; visualization, M.B.; supervision, M.B.; project administration, M.B. and J.S.; funding acquisition, M.B. and J.S. All authors have read and agreed to the published version of the manuscript.

Funding: This research received no external funding.

Institutional Review Board Statement: Not applicable.

Informed Consent Statement: Not applicable.

Data Availability Statement: Not applicable.

Conflicts of Interest: The authors declare no conflict of interest.

References

1. Zhang, N.; Zhao, R.; He, D.; Ma, Y.; Qiu, J.; Jin, C.; Wang, C. Lightweight and flexible Ni-Co alloy nanoparticle-coated electrospun polymer nanofiber hybrid membranes for high-performance electromagnetic interference shielding. *J. Alloys Comp.* **2019**, *784*, 244–255. [[CrossRef](#)]
2. Qian, K.; Yao, Z.; Lin, H.; Zhou, J.; Haidry, A. A.; Qi, T.; Chen, T.; Guo, X. The influence of Nd substitution in Ni–Zn ferrites for the improved microwave absorption properties. *Ceram. Int.* **2020**, *46*, 227–235. [[CrossRef](#)]
3. Stenglein, E.; Kohlhepp, B.; Kübrich, D.; Albach, M.; Dürbaum, T. GaN-half-bridge for core loss measurements under rectangular AC voltage and DC bias of the magnetic flux density. *IEEE Trans. Instrum. Meas.* **2020**, *69*, 6312–6321. [[CrossRef](#)]
4. Hoduń, P.; Borecki, M. Reliability Assessment of MV Power Connections. *Energies* **2021**, *14*, 6965. [[CrossRef](#)]
5. Lv, H.; Yang, Z.; Wang, P.L.; Ji, G.; Song, J.; Zheng, L.; Zeng, H.; Xu, Z.J. A voltageboosting strategy enabling a low-frequency, flexible electromagnetic wave absorption device. *Adv. Mater.* **2018**, *30*, 1706343. [[CrossRef](#)] [[PubMed](#)]
6. Suarez, A.; Victoria, J.; Torres, J.; Martinez, P.A.; Alcarria, A.; Perez, J.; Garcia-Olcina, R.; Soret, J.; Muetsch, S.; Gerfer, A. Performance Study of Split Ferrite Cores Designed for EMI Suppression on Cables. *Electronics* **2020**, *9*, 1992. [[CrossRef](#)]
7. Song, Y.-L.; Reddy, M.K.; Lin, H.-Y.; Chang, L.-M. Control of EMI in High-Technology Nano Fab by Exploitation Power Transmission Method with Ideal Permutation. *Appl. Sci.* **2021**, *11*, 11984. [[CrossRef](#)]
8. Dippong, T.; Levei, E.A.; Cadar, O. Preparation of CoFe₂O₄/SiO₂ Nanocomposites at low temperatures using short chain diols. *J. Chem.* **2017**, *2017*, 3. [[CrossRef](#)]
9. Baglio, S.; Caposciutti, G.; Marracci, M.; Tellini, B.; Trigona, C. Conception of a Temperature Sensor Based on 100-µm CoFeSiB Ferromagnetic Wire. *IEEE Trans. Instrum. Meas.* **2021**, *70*, 1–8. [[CrossRef](#)]
10. Dzikowski, L.; Tytko, G. A Method for Comparing the Metrological Properties of Eddy Current Probes. *IEEE Trans. Instrum. Meas.* **2021**, *70*, 1–6. [[CrossRef](#)]
11. Dippong, T.; Levei, E.A.; Tanaselia, C.; Gabor, M.; Nasui, M.; Barbu Tudoran, L.; Borodi, G. Magnetic properties evolution of the CoxFe_{3-x}O₄/SiO₂ system due to advanced thermal treatment at 700 °C and 1000 °C. *J. Magn. Magn. Mater.* **2016**, *410*, 47–54. [[CrossRef](#)]
12. Zheng, D.; Dong, Y. A Dual-parameter Oscillation Method for Eddy Current Testing with The Aid of Impedance Nonlinearity. *IEEE Trans. Instrum. Meas.* **2019**, *69*, 4476–4486. [[CrossRef](#)]
13. Vinnik, D.A.; Podgornov, F.V.; Zabeivorota, N.S.; Trofimov, E.A.; Zhivulin, V.E.; Chernukha, A.S.; Gavriyak, M.V.; Gudkova, S.A.; Zherebtsov, D.A.; Ryabov, A.V.; et al. Effect of treatment conditions on structure and magnetodielectric properties of barium hexaferrites. *J. Magn. Magn. Mater.* **2020**, *498*, 166190. [[CrossRef](#)]
14. Dippong, T.; Goga, F.; Levei, E.A.; Cadar, O. Influence of zinc substitution with cobalt on thermal behaviour, structure and morphology of zinc ferrite embedded in silica matrix. *J. Solid State Chem.* **2019**, *275*, 159–166. [[CrossRef](#)]
15. Vinnik, D.A.; Zhivulin, V.E.; Starikov, A.Y.; Gudkova, S.A.; Trofimov, E.A.; Trukhanov, A.V.; Trukhanov, S.V.; Turchenko, V.A.; Matveev, V.V.; Lahderanta, E.; et al. Influence of titanium substitution on structure, magnetic and electric properties of barium hexaferrites BaFe_{12-x}Ti_xO₁₉. *J. Magn. Magn. Mater.* **2020**, *498*, 166117. [[CrossRef](#)]
16. Trukhanov, A.V.; Astapovich, K.A.; Almessiere, M.A.; Turchenko, V.A.; Trukhanova, E.L.; Korovushkin, V.V.; Amirov, A.A.; Darwish, M.A.; Karpinsky, D.V.; Vinnik, D.A.; et al. Peculiarities of the magnetic structure and microwave properties in Ba(Fe_{1-x}Sc_x)₁₂O₁₉ (x < 0.1) hexaferrites. *J. Alloys Compd.* **2020**, *822*, 153575.
17. Borecki, M.; Sobolewski, K. An elimination method for an emergency situation in Gas-insulated switchgear in power grids. *IEEE Trans. Power Deliv.* **2021**, *36*, 3724–3732. [[CrossRef](#)]
18. Yang, Y.; Li, J.; Zhang, H.; Wang, G.; Rao, Y.; Gan, G. TiO₂ tailored low loss NiCuZn ferrite ceramics having equivalent permeability and permittivity for miniaturized antenna. *J. Magn. Magn. Mater.* **2019**, *487*, 165318. [[CrossRef](#)]
19. Huang, C.-C.; Mo, C.-C.; Chen, G.-M.; Hsu, H.-H.; Shu, G.-J. Investigation on the La Replacement and Little Additive Modification of High-Performance Permanent Magnetic Strontium-Ferrite. *Processes* **2021**, *9*, 1034. [[CrossRef](#)]
20. Takahashi, S.; Ogasawara, S.; Takemoto, M.; Orikawa, K.; Tamate, M. Experimental evaluation of the relationship between dimensional dependencies of MnZn ferrites and filter inductor impedances. *Electr. Eng. Jpn.* **2021**, *214*, e23302. [[CrossRef](#)]
21. Kruželák, J.; Kvasničáková, A.; Hložeková, K.; Plavec, R.; Dosoudil, R.; Gořalík, M.; Vilčáková, J.; Hudec, I. Mechanical, Thermal, Electrical Characteristics and EMI Absorption Shielding Effectiveness of Rubber Composites Based on Ferrite and Carbon Fillers. *Polymers* **2021**, *13*, 2937. [[CrossRef](#)] [[PubMed](#)]
22. Borecki, M.; Ciuba, M.; Kharchenko, Y.; Khanas, Y. Main aspects influencing the evaluation of atmospheric overvoltages in high-voltage networks. *Bull. Pol. Acad. Sci. Tech. Sci.* **2021**, *69*, e135838. [[CrossRef](#)]
23. Borecki, M. Risk level analysis in the selected (initial) stage of the project life cycle. *Manag. Prod. Eng. Rev.* **2020**, *11*, 104–112.
24. Borecki, M. A Proposed new approach for the assessment of selected operating conditions of the high voltage cable line. *Energies* **2020**, *13*, 5275. [[CrossRef](#)]
25. Borecki, M.; Sroka, J. Evaluation of the Effectiveness of Ferrite Characteristics Measurements Based on the CISPR 17 Standard. *IEEE Trans. Magn.* **2022**, *58*, 1–8. [[CrossRef](#)]